Title

Organized type I collagen influences endothelial patterns during “spontaneous angiogenesis in vitro”: Planar cultures as models of vascular development

Journal

In Vitro Cellular & Developmental Biology - Animal, 31(2)

ISSN

1071-2690

Authors

Vernon, Robert B
Lara, Stephanie L
Drake, Christopher J
et al.

Publication Date

1995-02-01

DOI

10.1007/bf02633972

Peer reviewed

In Vitro Cell. Dev. Biol. 31:120–131, February 1995

1071-2690/95 $02.50+0.00

ORGANIZED TYPE I COLLAGEN INFLUENCES ENDOTHELIAL PATTERNS DURING "SPONTANEOUS ANGIOGENESIS IN VITRO": PLANAR CULTURES AS MODELS OF VASCULAR DEVELOPMENT

ROBERT B. VERNON[1], STEPHANIE L. LARA, CHRISTOPHER J. DRAKE, M. LUISA IRUELA-ARISPE, JOHN C. ANGELLO, CHARLES D. LITTLE, THOMAS N. WIGHT, AND E. HELENE SAGE

Departments of Biological Structure (R. B. V., E. H. S.), Pathology (S. L. L., T. N. W.), and Biochemistry (J. C. A.), University of Washington, Seattle, Washington 98195; Department of Cell Biology and Anatomy (C. J. D., C. D. L.), Medical University of South Carolina, Charleston, South Carolina 29425; and Department of Pathology (M. L. I.-A.), Beth Israel Hospital/Harvard Medical School, Boston, Massachusetts 02215

(Received 9 June 1994; accepted 4 August 1994)

SUMMARY

Selected strains of vascular endothelial cells, grown as confluent monolayers on tissue culture plastic, generate flat networks of cellular cords that resemble beds of capillaries—a phenomenon referred to as "spontaneous angiogenesis in vitro". We have studied spontaneous angiogenic activity by a clonal population (clone A) of bovine aortic endothelial cells to indentify processes that mediate the development of cellular networks. Confluent cultures of clone A endothelial cells synthesized type I collagen, a portion of which was incorporated into narrow, extracellular cables that formed a planar network beneath the cellular monolayer. The collagenous cables acted as a template for the development of cellular networks: flattened, polygonal cells of the monolayer that were in direct contact with the cables acquired spindle shapes, associated to form cellular cords, and became elevated above the monolayer. Networks of cables and cellular cords did not form in a strain of bovine aortic endothelial cells that did not synthesize type I collagen, or when traction forces generated by clone A endothelial cells were inhibited with cytochalasin D. In a model of cable development, tension applied by a confluent monolayer of endothelial cells reorganized a sheetlike substrate of malleable type I collagen into a network of cables via the formation and radial enlargement of perforations through the collagen sheet. Our results point to a general involvement of extracellular matrix templates in two-dimensional (planar) models of vascular development in vitro. For several reasons, planar models simulate invasive angiogenesis poorly. In contrast, planar models might offer insights into the growth and development of planar vascular systems in vivo.

Key words: endothelial cell; angiogenesis; vasculogenesis; in vitro; extracellular matrix; collagen.

INTRODUCTION

The growth of new vascular sprouts from extant vasculature, referred to as angiogenesis, is an important component of wound repair, tumor growth, and a variety of other normal and pathologic processes in vivo. The morphogenetic and regulatory processes that mediate and control angiogenesis are difficult to visualize and to manipulate in vivo. Therefore, investigators have developed models in which isolated endothelial cells are grown in vitro under conditions that promote their organization into multicellular structures that resemble networks of microvasculature (3,8–10,16–21,23,26,27,29–32). Certain populations of endothelial cells, maintained as confluent monolayers for 2 to 4 wk on unmodified tissue culture plastic, generate a network of cellular cords—a phenomenon that has been termed "spontaneous angiogenesis in vitro" (3,8,9,16–19). It has been assumed that the spontaneous appearance of endothelial cord networks in vitro is an adequate model, in terms of morphology, of angiogenesis in vivo. Consequently, studies of spontaneous angiogenesis in vitro have focused on molecular phenomena that include the expression of specific proteins and mRNA by cells in the networks or the influence of specific molecules (e.g., growth factors) on the formation of networks (3,16–19). In contrast, it has not been adequately determined whether the changes in cellular morphology and orientation that characterize spontaneous angiogenesis in vitro are indeed consonant with angiogenesis in vivo. In the present study, we examine key morphologic events of spontaneous angiogenesis in vitro exhibited by a clonal population of bovine aortic endothelial cells (BAECs). We find that the spatial organization of cells in the model is atypical of angiogenesis in vivo. Moreover, we observe that endogenously synthesized extracellular matrix (ECM) mediates the formation of the endothelial cord networks. We conclude that models of spontaneous angiogenesis in vitro are of limited use in studies of angiogenesis in vivo; however, we introduce the concept of planar models of vascular development and we propose that planar models might be useful in understanding the development of vasculature with planar characteristics in vivo.

[1] Department of Biological Structure, SM-20 University of Washington Seattle, WA 98195.

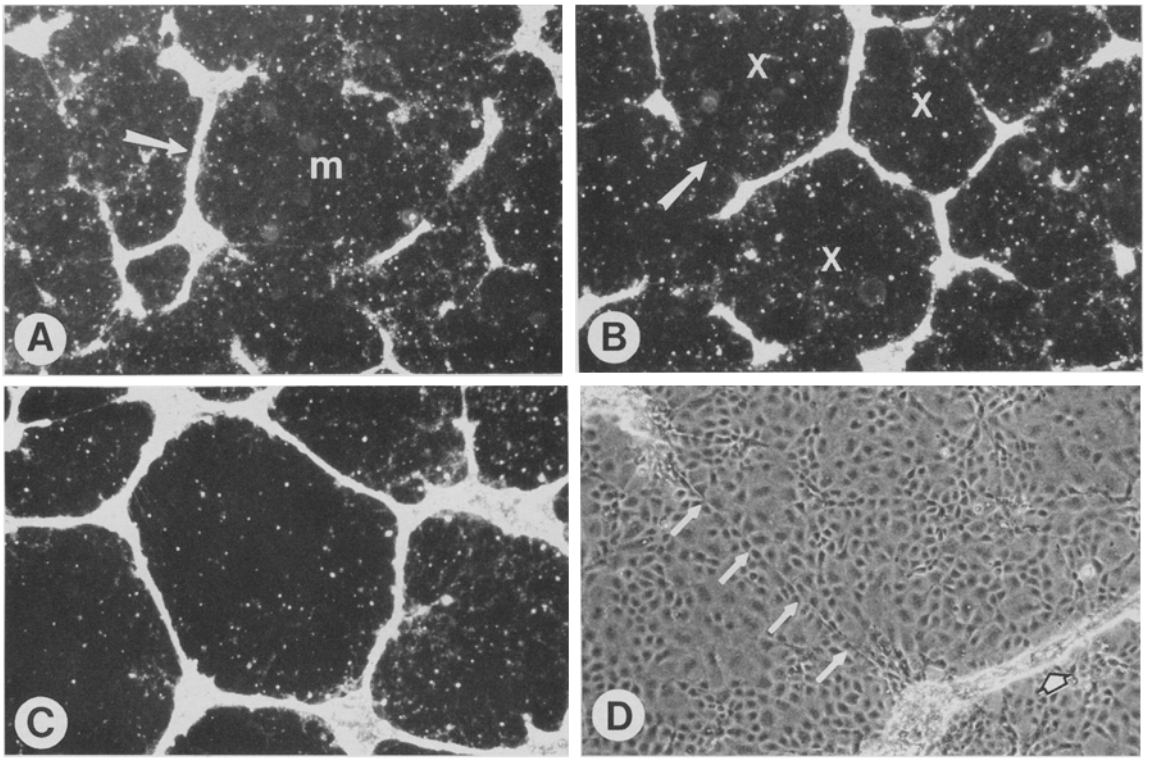

FIG. 1. BAECs form cellular networks spontaneously on plastic substrates. *A*, 6 days after becoming confluent on tissue-culture plastic, a monolayer (*m*) of clone A BAECs generates short cords of cells (e.g., *arrow*) that are visible as bright areas in this low magnification, darkfield image. *B*, after 10 days, cords are organizing into polygonal tesserae. Geometric centers (*X*) of three tesserae with incomplete boundaries are indicated. *C*, in another area of the culture shown in *B*, all boundaries of tesserae are defined by cellular cords, each of which is formed from many cells. *D*, one incomplete boundary, indicated by an *arrow* in *B*, is enlarged. Although a cellular cord has not yet formed, the boundary is defined by a narrow, linear track of refractile, extracellular material (*thin arrows*) that intersects an adjacent cellular cord (*broad arrow*). *D*, phase contrast (×95); all other images are darkfield (×24).

MATERIALS AND METHODS

Cells and cell culture. BAECs were isolated from adult aortae by treatment with 0.5% trypsin in versene and were grown in 75-cm^2 plastic tissue culture flasks in Dulbecco's modified Eagle's medium (DMEM) with 10% fetal bovine serum (FBS) (Hyclone Laboratories, Logan, UT), 100 U/ml penicillin G, 100 μg/ml streptomycin SO_4, and 250 μg/ml amphotericin B. After 1 wk, cells were replated at a high dilution (1 cell/well) in 96-well plastic tissue culture plates and maintained in culture medium that was preconditioned by a 1-wk exposure to confluent BAECs. Clonal colonies were subcultured, analyzed for uptake of acetylated low-density lipoprotein and expression of von Willebrand factor, and monitored for the presence of cellular networks. One clone (clone A) formed well-defined networks in vitro and was selected for further study. In studies of spontaneous formation of cellular networks, BAECs were cultured in unmodified 75-cm^2 tissue culture flasks in DMEM/10% FBS. In studies of reorganization of exogenous substrates of collagen, BAECs were grown on layers of gelled, bovine type I collagen made from Vitrogen (Celtrix Corp., Palo Alto, CA). Vitrogen (3 mg/ml) was combined with 1/6 vol of 7× DMEM, adjusted to 0.32 mg/ml collagen with DMEM, dispensed into 35-mm tissue culture wells, and gelled at 37° C.

Light and electron microscopy. Cell cultures were examined routinely by phase contrast light microscopy, dark field illumination, and time-lapse videomicroscopy (40). Cultures in 75-cm^2 flasks were prepared for scanning electron microscopy (SEM) by fixation for 1 h at room temperature with 3% glutaraldehyde in 0.1 *M* Na cacodylate/4% sucrose buffer (pH 7.4). Cultures were postfixed for 30 min with 1% OsO_4 in 0.1 *M* phosphate buffer, pH 7.4. Squares of 10 to 15 mm were cut from the bottoms of the culture flasks, dehydrated, coated with gold-palladium, and viewed with a JSM 6300F field emission scanning electron microscope at 15 kV. For analyses by transmission electron microscopy (TEM), cultures in 75-cm^2 flasks were fixed in half-strength Karnovsky solution, postfixed with 1% OsO_4 in 0.1 *M* Na cacodylate buffer (pH 7.4), dehydrated, and embedded in Epon in situ. Thin (80 to 100 nm) sections were stained with uranyl acetate/lead citrate and were viewed with a JEOL 1200 EXII at 80 kV.

Collagen gel contraction assay. The ability of BAECs to reorganize fibrils of type I collagen was analyzed with a collagen gel contraction assay (1,11,12,38). Wells of a 24-well tissue culture plate were made nonadhesive with a thin layer of 1% agarose (Sea-Kem LE; FMC BioProducts, Rockland, ME). Solutions were prepared from Vitrogen as described previously to yield gels with final collagen concentrations of 1, 0.75, 0.5, 0.375, or 0.25 mg/ml. One volume of DMEM that contained suspended BAECs at 3×10^6/ml was combined with 9 vol of type I collagen solution. The mixtures were made 2% with FBS, dispensed into the agarose-coated wells (500 μl/well), and gelled for 2 h at 37° C. Five-hundred microliters of DMEM with 2% FBS and antibiotics were then added to each well to float the collagen disks. After incubation of the plate for 18 h at 37° C, the degree of contraction of each disk was determined as described by Gullberg et al. (12), i.e., by measurement of the diameter of the cellular ring that formed at the periphery of the gel as a consequence of the contraction process.

Protein analyses and immunohistochemistry of cultured BAECs. BAECs cultured in 75-cm^2 flasks were incubated 19 h in DMEM that contained 50 μCi/ml of L-[2,3,4,5-^{3}H] proline (Amersham, Arlington Heights, IL). Medium that contained secreted proteins was collected, supplemented with a mixture of protease inhibitors, centrifuged to remove particulate matter, dialyzed 72 h against 0.5 *N* acetic acid, and lyophilized. Lyophilized proteins were resuspended in Laemmli buffer (24), reduced with 10 m*M* dithiothreitol, resolved by sodium dodecyl sulfate-polyacrylamide gel electrophoresis (SDS-PAGE), and visualized by autoradiofluorography (17). In Western blot analyses, proteins lyophilized from culture media (not

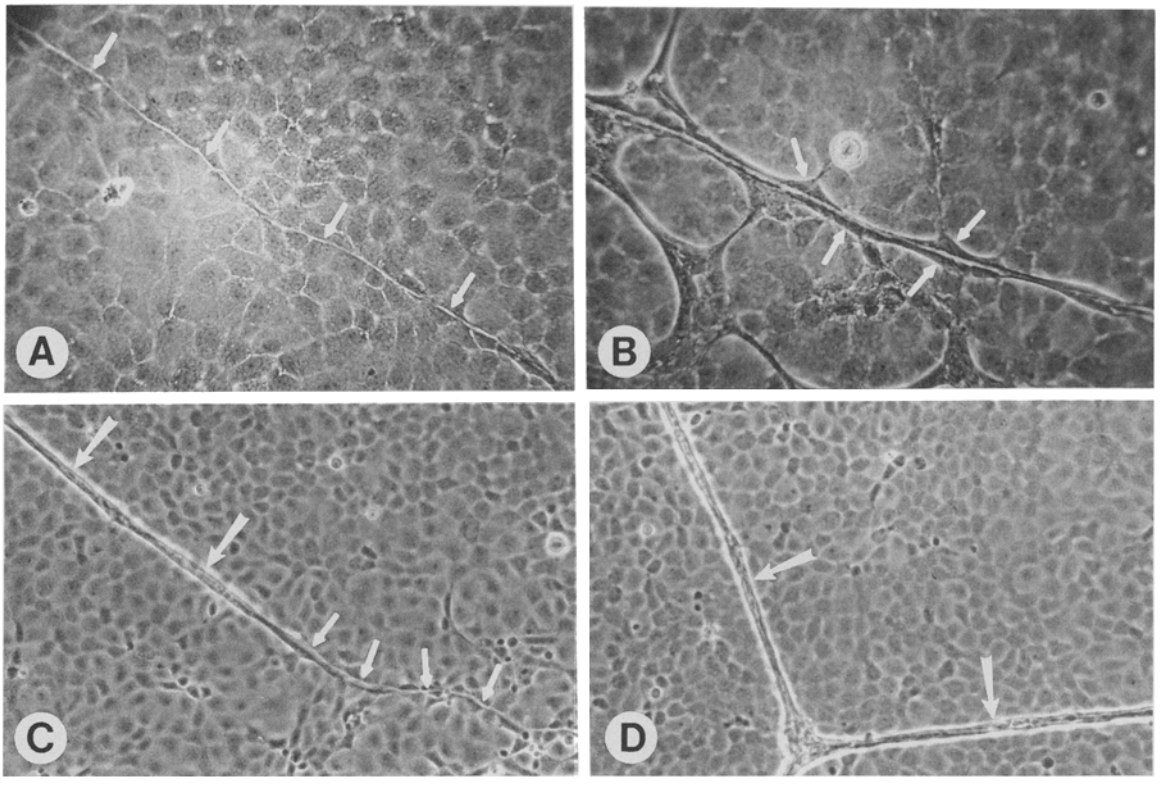

FIG. 2. Cellular cords form on extracellular tracks. *A*, before development of cellular cords, linear tracks of refractile extracellular material (one track is indicated by *arrows*) first appear among the flattened, polygonal cells of the monolayer. *B*, with time, cells (*arrows*) in direct contact with the tracks assume elongated, spindle/polygonal shapes. *C*, eventually, tracks (one is indicated by *small arrows*) become obscured in segments by narrow cords of elongate, refractile cells (a cellular cord is indicated by *large arrows*). *D*, process is complete when tracks are fully hidden by cellular cords. Here, two cellular cords (*arrows*) intersect. *A–D*, phase contrast. *A,B* (×240); *C,D* (×120).

supplemented with ^{3}H-proline) were resolved by SDS-PAGE, transferred to nitrocellulose membranes, immunolabeled (41) with antiserum against type I collagen, exposed to ^{125}I-protein A (DuPont-NEN, Boston, MA), and visualized by autoradiography. For immunohistochemical assays, cultures of clone A BAECs were fixed in 2% formaldehyde/phosphate buffered saline (PBS); squares of 20 mm were cut from the bottoms of the culture flasks, washed in PBS, blocked 30 min in PBS/2% normal rabbit serum, and exposed to antiserum against type I collagen. Bound antibodies were visualized with a Vectastain avidin-biotin-peroxidase kit and 3,3′-diaminobenzidine-4HCl (Vector Laboratories, Burlingame, CA). Antiserum against type I collagen was generated by immunization of guinea pigs with type I collagen that was purified from lathyritic rat skin. Titer and specificity of the antibodies were determined by enzyme-linked immunoadsorbent assays and Western blot analyses of both purified collagen and conditioned media from cultured fibroblasts (17).

Imaging of vasculogenesis in developing quail. Early stage (6 to 8 somite) Japanese quail embryos (*Coturnix coturnix japonica*) and surrounding vitelline membranes were isolated from yolks by use of filter paper rings (7). The rings (i.d. 6 mm, o.d. 12 mm) served as frames that supported the embryos for immunolabeling and imaging. Ring/embryo assemblies were fixed, permeabilized, exposed to culture supernate from the QH1 murine hybridoma (Developmental Studies Hybridoma Bank, University of Iowa), and labeled with a fluorescein isothiocyanate-conjugated, goat anti-mouse secondary antibody (7). The QH1 antibody is considered a marker for primordial endothelial cells (34). Immunolabeled ring/embryo assemblies were mounted on slides and optically sectioned at 5 μm with a scanning laser confocal microscope (Bio-Rad MRC 1000). Images were formed by a computer-generated superposition of 10 optical sections (made serially along the Z axis) that were scanned in the XY plane.

RESULTS AND DISCUSSION

Spontaneous formation of BAEC networks in vitro: examination by light microscopy. Clone A BAECs maintained on tissue culture plastic in the presence of 10% FBS proliferated to form confluent monolayers. Approximately 4 days after cultures had attained confluence, short, cordlike arrays of refractile cells appeared among the flattened cells of the monolayer. Within 6 to 10 days, the cellular cords had lengthened considerably and had established connections with one another to form tessellated networks (Fig. 1 *A–C*). Cellular cords that formed the sides of tesserae were comprised of a variable number of cells. In some cases, however, one or more sides of tesserae lacked cells but were nonetheless demarcated by narrow, refractile lines that ran in straight, uninterrupted courses (Fig. 1 *D*). Henceforth, we refer to the refractile lines as "tracks".

Daily examination of confluent clone A BAEC cultures revealed that the refractile tracks appeared spontaneously among the flattened, polygonal cells of the monolayers (Fig. 2 *A*). With time, cells that made direct contact with tracks became rounded and acquired bipolar shapes in parallel with the long axes of the tracks (Fig. 2 *B*). Eventually, tracks became obscured, either in segments or in toto, by narrow cords of elongate, refractile cells (Fig. 2 *C,D*). Time-lapse light videomicroscopy confirmed that: a) cellular cords arose as a consequence of shape changes by cells in contact with previously formed tracks, b) divisions were rare among cells in cords and cells of the monolayer, and c) directional migration by cells was restricted to very slow, intermittent movement along tracks.

Examination of BAEC networks by SEM and TEM. SEM images revealed that monolayers of clone A BAECs were comprised of flattened polygonal cells, the borders of which were closely juxtaposed and indistinct in areas where shrinkage had not pulled adja-

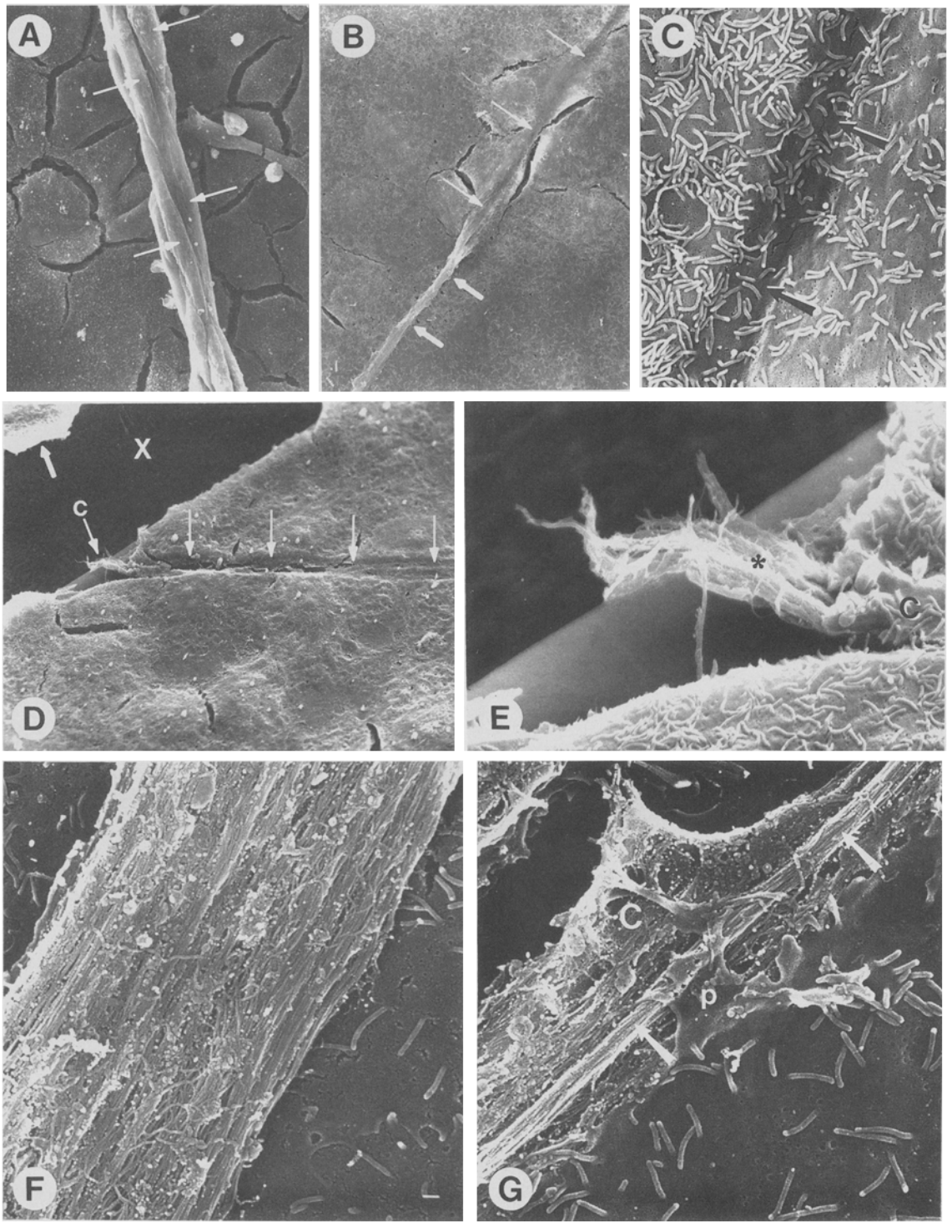

FIG. 3. Analysis by SEM of tracks and cellular cords formed by clone A BAECs. *A*, spindle-shaped cells (*arrows*) form a cord that runs on top of a monolayer of flattened cells. *B*, linear track of extracellular material (*arrows*) associates with the cellular monolayer. Portions of the track run either beneath (*thin arrows*), or above (*thick arrows*), the monolayer. *C*, a dark, linear track (*arrows*) that runs beneath the cellular monolayer is viewed at high magnification. Track is covered by the margins of flattened cells, which bear microvilli. *D*, a track similar to the one in *C*, but viewed at 60° of tilt, appears as a shallow groove (*thin arrows*) in the monolayer of cells. Track has been transected by a large crack (*X*) that developed in the plastic of the culture dish during preparation of the specimen. Near the edge of the crack, a small portion of the cable of ECM (*c*) that forms the track has been exposed. The ECM was originally covered by a flattened cell (*thick arrow*). *E*, exposed cable of ECM in *D* is viewed at a higher magnification. Cable (*asterisk*), which protrudes from beneath a cell (*c*), is comprised of fibrous material. *F*, a large cable of ECM that lies above the cellular monolayer is comprised of bundles of parallel filaments. *G*, a cable (*C*) of ECM emerges from beneath the cellular monolayer. A prominent bundle of fibers (*arrows*) is contacted by a cellular process (*p*). *A* (×740), *B* (×985), *C* (×7360), *D* (×1030), *E* (×6520), *F,G* (×11400).

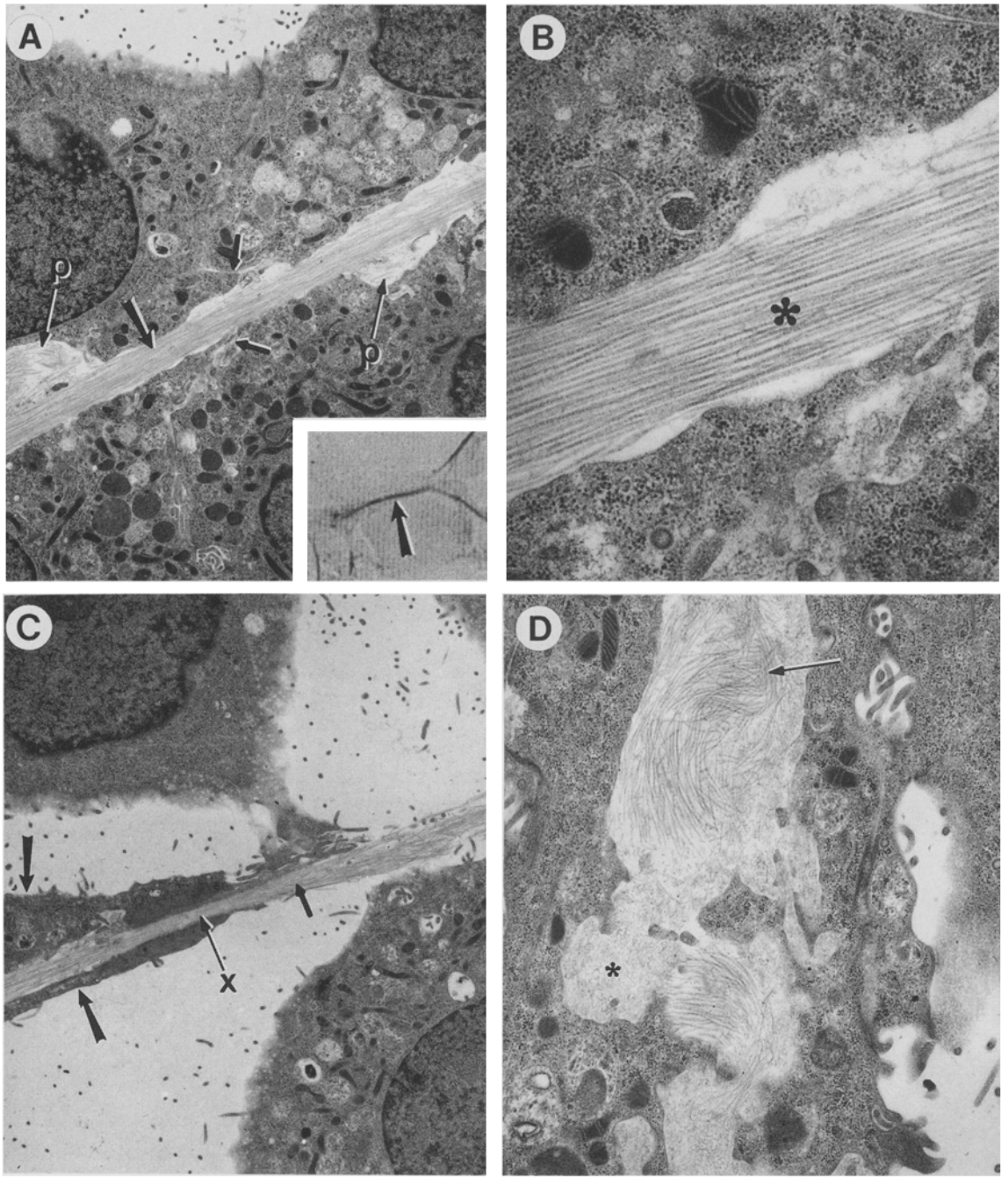

FIG. 4. Analysis of spontaneously formed networks by TEM. *A–D* are sections of cord-forming cultures that were cut parallel to the plane of the culture dish. *A*, a cable of ECM (*large arrow*), formed primarily from aligned fibrils of collagen, courses through the cellular monolayer. Cells make contact with the cable via irregular borders. Continuity of the collagen fibers within the cable is not interrupted at intercellular junctions (*small arrows*). At intervals, extracellular pockets (*p*) contain collagen fibers and fibrillogranular material. A similar cable (*inset*) has bound antibodies to type I collagen and is revealed by diaminobenzidine as a dark line (*arrow*) in this light micrograph. *B*, cable of ECM in the center region of *A* is enlarged. Cable (*asterisk*) is comprised of banded fibrils of collagen that are closely associated and aligned. *C*, a spindle-shaped endothelial cell (*large arrows*) associates with a cable of collagen fibers (*small arrow*) that runs above the cellular monolayer. In one segment of the cable (*X*), collagen fibers are closely packed, perhaps due to compression forces exerted by the cell. *D*, a large extracellular space, not associated with extracellular cables, contains fibrillogranular material (*asterisk*), and twisted, loosely bundled fibers of collagen (*arrow*). *A–D* are ×6450, ×32 000, ×6450, and ×15 000, respectively. *Inset* is ×800.

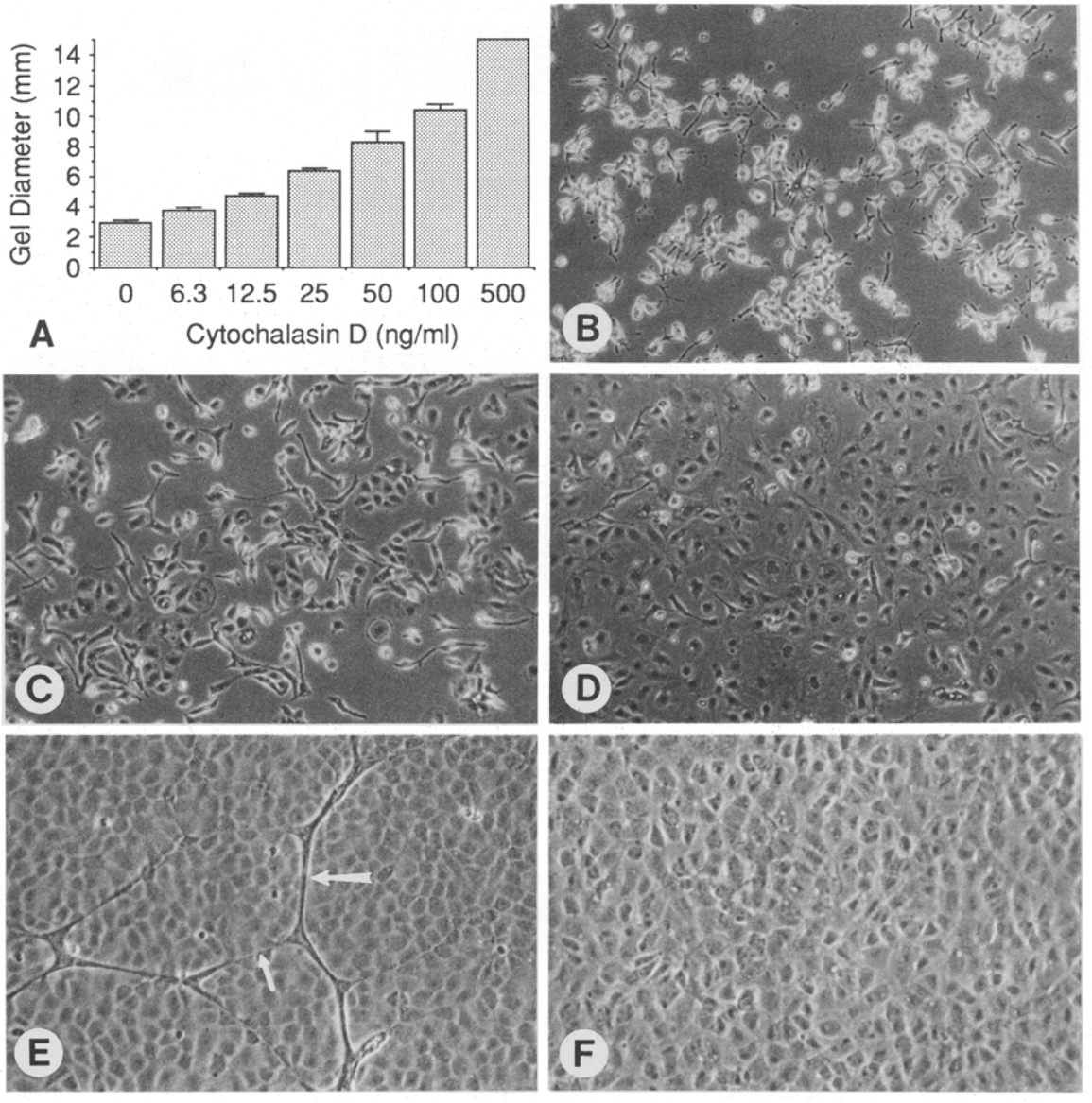

FIG. 5. Disruption of microfilaments in clone A BAECs with cytochalasin D inhibits cellular traction and the spontaneous formation of networks. *A*, clone A BAECs, embedded in 15-mm disks of malleable (0.375 mg/ml) type I collagen, were cultured for 18 h in various concentrations of cytochalasin D. Cell-induced contraction of the disks is inhibited in a dose-dependent manner by the drug (results are expressed as the average of five replicates with standard deviations indicated by *T-bars*). *B–D*, BAECs plated onto plastic substrates and cultured for 6 h in the presence of cytochalasin D. *B*, in 500 ng/ml cytochalasin D, spreading is significantly inhibited. Spreading improves in 100 ng/ml (*C*) or 12.5 ng/ml (*D*) of the drug. *E*, after 7 days in 6.3 ng/ml cytochalasin D, confluent clone A BAECs are forming tracks (*small arrow*) and cellular cords (*large arrow*). *F*, after 7 days in 75 ng/ml of the drug, confluent clone A BAECs remain spread but do not form networks. *B–F*, phase contrast (×120).

cent cells away from one another. The upper surfaces of the cells were devoid of deposits of ECM and were covered with short microvilli. Cellular cords, which formed a network that lay on the upper surface of the monolayer, were comprised of spindle-shaped cells with few or no microvilli (Fig. 3 *A*). In addition to cellular cords, some portions of the network consisted of narrow, linear structures that were interpreted to be the tracks visible with the light microscope (Fig. 3 *B*). Tracks frequently appeared as dark, shallow depressions in the surface of the cellular monolayer (Fig. 3 *C,D*). The depressed areas were covered by polygonal cells with morphologies that were not obviously different from cells in areas removed from the tracks. Tracks that were transected during preparation for SEM exhibited cablelike, fibrous extracellular material beneath the cells (Fig. 3 *D,E*). Occasionally, intact extracellular cables emerged from beneath the cellular monolayer to run above the monolayer (Fig. 3 *B*). In these instances, the fibrous structure of the cables was clearly evident (Fig. 3 *F,G*).

The structure of the cables and associated cells was examined at higher resolution by TEM. Cables consisted primarily of long, highly aligned fibers of ECM that, based on their size and pattern of banding, seemed to be type I collagen (Fig. 4 *A–C*). The presence of type I collagen within tracks was verified by labeling with specific

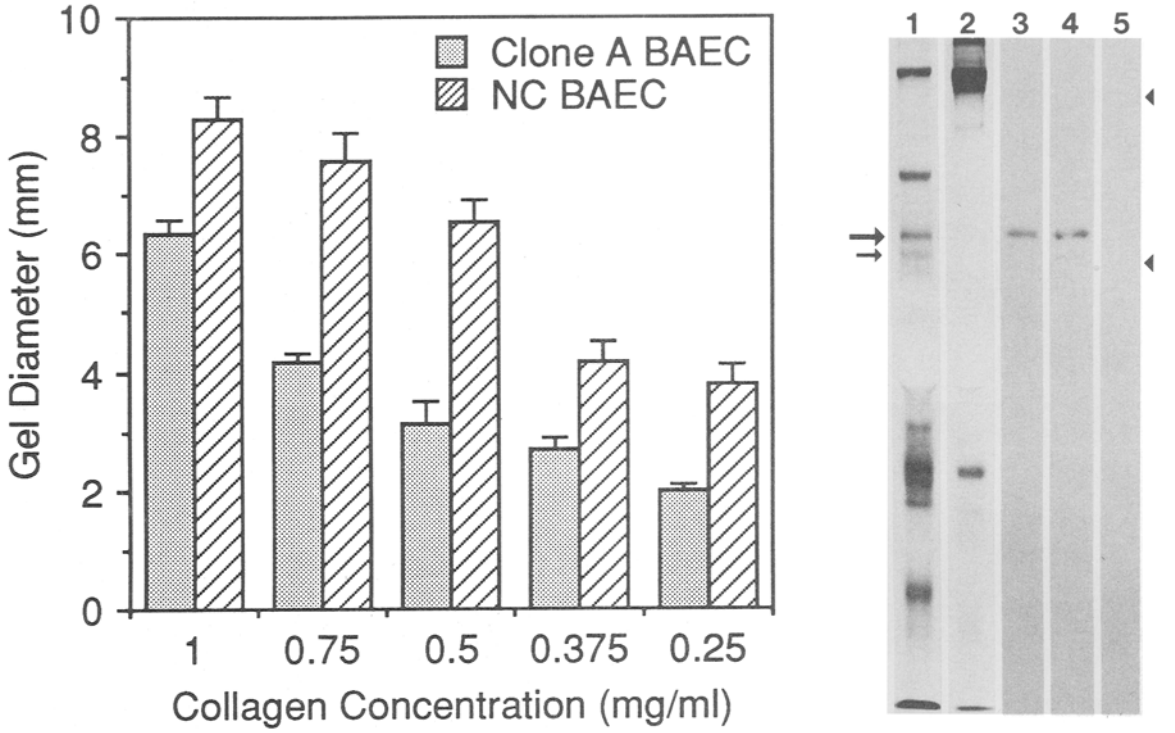

FIG. 6. Clone A and NC BAECs differ in the ability to reorganize and synthesize type I collagen. Equal numbers of clone A BAECs and NC BAECs were tested in a collagen gel contraction assay (*bar graph*). After 18 h in vitro, clone A BAECs had contracted disks of 15 mm diameter formed from different concentrations of collagen to a greater degree than did NC BAECs (results are expressed as the average of five replicates with standard deviations indicated by *T-bars*). Analyses of type I collagen by SDS-PAGE are shown at right in *lanes 1–5*. [^{3}H]proline-labeled proteins synthesized by clone A BAECs (*lane 1*) and NC BAECs (*lane 2*) were visualized by autoradiography. Bands corresponding to α1(I) and α2(I) chains of type I collagen (*large* and *small arrows*, respectively) were synthesized by clone A BAECs but not by NC BAECs. The α1(I) chain was prominent in immunolabeled Western blots of proteins synthesized by clone A BAECs (*lane 3*) and a standard of type I collagen purified from rat dermis (*lane 4*), but was not observed in blots of NC BAEC proteins (*lane 5*). *At far right*, upper and lower *arrowheads* indicate the position of molecular weight standards (globular proteins) of 200 and 97 kDa, respectively.

antibodies (Fig. 4 *A inset*). Cells contacted the cables of collagen via irregular borders that frequently were indented by large pockets (Fig. 4 *A*). The pockets contained fibrillogranular material and poorly organized, often twisted bundles of collagen. ECM of a similar composition was deposited in areas that were not associated with cables (Fig. 4 *D*). Regions of cables that passed by pockets showed little or no splaying of the aligned collagen fibers. Moreover, collagen fibers within cables did not exhibit discontinuities as they ran past intercellular junctions.

Studies of ECM reorganization in vitro. Subconfluent cells apply tensile forces to layers of malleable ECM in vitro that can cause the ECM to reorganize into networks of cables (40); therefore, it was possible that cellular tension played a role in the development of collagenous networks beneath confluent monolayers of clone A BAECs. Cells apply tension to ECM as they pull ECM toward them via a process referred to as traction (13,14,39,40) which is manifested as a shearing force that acts at a tangent to the surfaces of cells (39). The generation of forces of cellular traction requires cytoplasmic microfilaments (39,40); therefore, we examined the consequences of disruption of microfilaments (with cytochalasin D) on the spontaneous development of ECM tracks by clone A BAECs. Forces of traction that cells (e.g., fibroblasts) apply to collagen can be compared by measuring cell-driven contraction of disk-shaped collagen gels (1,11,12,38). We employed such an assay to determine how graded doses of cytochalasin influenced clone A BAECs. Traction that clone A BAECs applied to collagen in the absence of cytochalasin D was surprisingly strong: disks of collagen were contracted up to one-tenth of their original diameter over a period of 18 h. In fact, clone A BAECs remodeled collagen gels more effectively than did fibroblasts from fetal bovine ligament (not shown). Cytochalasin D inhibited the contraction of collagen gels by clone A BAECs in a dose-dependent manner (Fig. 5 *A*): complete inhibition was achieved with 500 ng/ml of the drug. Inhibition was reversible: disks were fully contracted 24 h after the cytochalasin was washed

FIG. 7. Confluent monolayers of BAECs reorganize sheets of malleable type I collagen into networks of cables that resemble networks generated spontaneously in vitro. *A*, a gel of type I collagen has become perforated after 10 days beneath a confluent monolayer of NC BAECs. Two large perforations (*X*) are indicated. *B*, perforations are more easily seen when the collagen gel of *A* is rendered as a tracing (*gray stipple*), with the cellular monolayer not shown. Perforations (*white profiles*) are roughly circular and vary greatly in size. With time, perforations enlarge and coalesce as the collagen between them thins and ruptures (*arrows*). *C*, after 14 days,

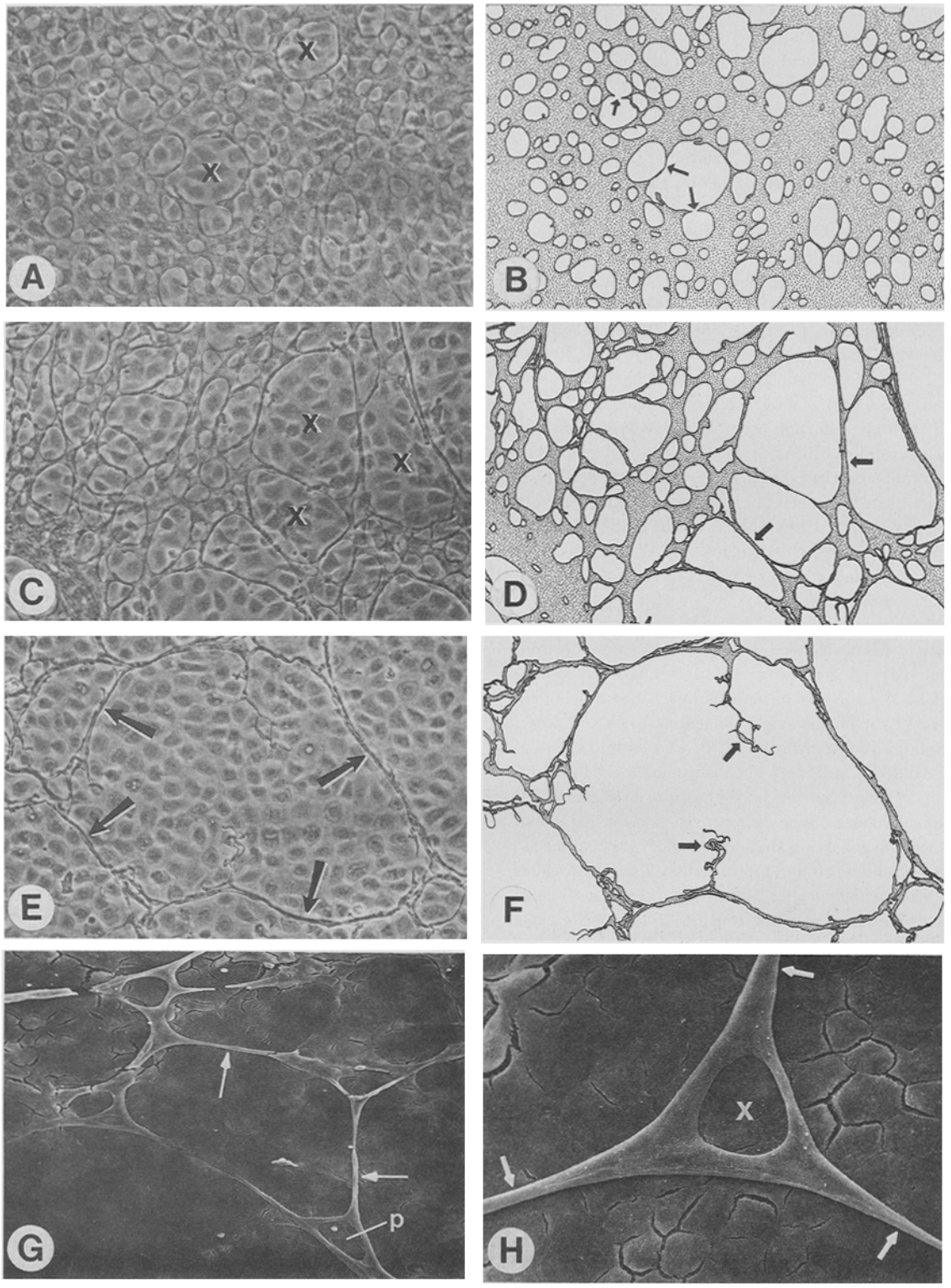

larger, polygonal perforations (*X*) are observed. *D*, tracing of collagen gel shown in *C*. Sheetlike areas of collagen bear small, circular perforations. Collagen between larger, polygonal perforations is formed into cables (*arrows*). *E*, after 18 days, cables of collagen (*arrows*) define the boundaries of a large polygon. *F*, tracing of collagen gel shown in *E*. *Arrows* indicate the two retracted ends of a cable of collagen broken by forces of tension. This cable, when intact, divided the large polygon into two smaller areas. *G*, confluent monolayers of clone A BAECs, cultured on plastic, generate networks that resemble the reorganized collagen gels in *A–F*. Cables of ECM (*arrows*), ensheathed by cells, form the sides of large polygons. Vertex areas are perforated by smaller, circular openings. One such perforation (*p*) is indicated. *H*, from culture shown in *G*, three cables (*arrows*) of cells and ECM intersect above the cellular monolayer. Sheetlike area of intersection (vertex) bears a circular perforation (*X*). *A,C,E*, phase contrast (×120); *G*, SEM (60° tilt) (×128); *H*, SEM (×490).

from assay wells. Levels of cytochalasin that inhibited the contraction of gels by clone A BAECs clearly affected the cytoskeleton because microfilament-dependent spreading of the cells on plastic substrates was also inhibited (Fig. 5 *B–D*). Confluent cultures of clone A BAECs developed networks of ECM after 7 days of exposure to low levels of cytochalasin D (Fig. 5 *E*), but moderate levels of the drug inhibited development of ECM networks (Fig. 5 *F*). ECM networks appeared in inhibited cultures within 7 days after the drug was washed away (not shown).

A strain of BAECs termed "NC" (i.e., "non-cord-forming"), isolated from the same aorta as clone A BAECs, lacked the ability to form networks of cells and ECM spontaneously. We compared clone A BAECs to NC BAECs with respect to levels of collagen synthesis and gel contraction to explore the relationship between spontaneous networks and synthesis/reorganization of type I collagen by cells. The ability of NC BAECs and clone A BAECs to contract a series of collagen gels with increasing malleabilities (established by a stepwise reduction of collagen concentration) was examined. For both strains of BAECs, gel contraction increased as collagen concentration decreased (Fig. 6, *graph*). Clone A BAECs, however, had contracted collagen at all levels of malleability to a greater degree than did NC BAECs. Analyses by SDS-PAGE and Western blot methods revealed that clone A BAECs synthesized type I collagen as expected, whereas NC BAECs did not synthesize this protein (Fig. 6, *lanes 1–5*).

Our morphologic observations and gel contraction data suggested to us that tension forces developed by clone A BAECs were involved in the organization of endogenously synthesized collagen into a network-like scaffold. It was not clear to us, however, how a confluent monolayer of BAECs might remodel collagen into such a network; therefore, we cultured monolayers of NC BAECs on thin layers of malleable (0.32 mg/ml), gelled type I collagen and looked for conversion of the unorganized collagen into network-like structures. NC BAECs grew to confluence on the collagen gels and formed monolayers of flattened polygonal cells that were similar in appearance to monolayers on a plastic substrate. Approximately 7 to 10 days after the cultures became confluent, the homogeneous, planar sheet of collagen developed an array of small, roughly circular perforations (Fig. 7 *A,B*). With time, the perforations enlarged, coalesced, and assumed polygonal shapes. As the perforations enlarged, the collagen that surrounded them was remodeled from a sheet into a network of narrow cables (Fig. 7 *C–F*), a process that was blocked by moderate levels (i.e., 75 to 100 ng/ml) of cytochalasin D (not shown). Low-magnification SEM images of clone A BAEC cultures indicated that networks of endogenously synthesized ECM arose in a similar fashion, i.e., via a conversion of sheets of ECM into cables by the enlargement of circular perforations (Fig. 7 *G,H*).

Type I collagen guides the organization of endothelial cells in spontaneous angiogenesis in vitro. Inherent difficulties in the isolation and definition of specific cellular and biochemical events in vivo have made it highly desirable to establish experimental models of angiogenesis in vitro. Several methods of endothelial cell culture generate multicellular structures with network-like characteristics of microvasculature. In some culture systems, microvascular endothelial cells invade relatively thick substrates of type I collagen and form cords and tubes that branch and anastomose in three dimensions (29–32). In contrast, cellular invasion plays little or no role in the spontaneous model described in the present study: instead, a confluent monolayer of endothelial cells generates an overlying two-dimensional network of cellular cords. Previous studies had shown a correlation between synthesis of type I collagen in situ and spontaneous angiogenesis in vitro (6,17,18); however, a specific function for the collagen in the development of cellular cord networks remained undefined. Our results indicate that the type I collagen secreted by the endothelial monolayer becomes organized into a scaffold-like network of aligned fibers. The collagenous scaffold is colonized by endothelial cells that subsequently elongate and form cords. Accordingly, a strain of BAECs ("NC") that does not synthesize type I collagen lacks the ECM scaffold and does not generate endothelial networks. Our results suggest that tensile forces developed by the endothelial monolayer are important in the organization of type I collagen into the scaffold. In this regard, it is interesting that NC BAECs are less effective at remodeling extant type I collagen than are clone A BAECs (as indicated by differences in capability to contract collagen gels). We find that dermal fibroblasts from embryonic mice that lack the ability to synthesize type I collagen (i.e. the mice are homozygous for the *mov 13* defect, which specifically blocks transcription of the type I collagen gene) are significantly weaker contractors of type I collagen gels than are normal, wild-type embryonic dermal fibroblasts that synthesize the protein (Iruela-Arispe, Vernon, and Sage, manuscript in preparation); therefore, the potential exists for newly synthesized collagen to promote cellular behaviors that lead to collagen reorganization.

Planar arrangements of cells and ECM promote the formation of networks in vitro. The presence of an ECM scaffold is a characteristic that relates our model of spontaneous angiogenesis to certain other models of angiogenesis in vitro. For example, the formation of cellular networks by subconfluent endothelial cells cultured on Matrigel (a gel of basement membrane components) in vitro has been proposed as a model of angiogenesis in vivo (10,23). In studies of the Matrigel model, we found that ECM scaffolds were critical to the development of the cellular networks: endothelial cells aligned the Matrigel into a network of narrow cables that acted as a "template" on which a network of endothelial cords developed (40).

We find it significant that even though the Matrigel and spontaneous models differ with respect to type and origin of ECM (i.e. exogenous basement membrane components that lack type I collagen vs. type I collagen synthesized by the endothelial cells in situ) and with respect to cellular density (i.e. the spontaneous model requires confluency: the Matrigel model does not), both models utilize ECM scaffolds to generate cellular cord networks. A critical point of similarity between the two models seems to be the planar nature of the cells and ECM—an arrangement that facilitates the generation of network-like patterns (Fig. 8). In planar cultures, cells act as traction centers that pull ECM toward them in a continuous manner (13,14,33,39,40,42) and establish radiating lines of strain (traction fields) in the ECM (39) (Fig. 8 *A*). Where adjacent traction fields overlap, tension in the ECM is enhanced (the two-center effect) (14,15,42) (Fig. 8 *B*) which causes fibers of ECM to align into narrow cables or tracks that connect the traction centers (Fig. 8 *C*). Networks of aligned ECM form when multiple two-center effects are established among neighboring traction centers (40) (Fig. 8 *D*). In situations where ECM is highly malleable, centripetal movement of ECM to traction centers can result in the reorganization of ECM into a web of cables via perforation of the ECM sheet (Fig. 8 *E*). Scaffold-like structures of ECM seem to be present in yet another model of vascular development in vitro: the induction of endothelial networks from endothelial monolayers by dilute suspensions of type I collagen fibers (20,21). It seems to us that cell/ECM networks in this particular model resemble networks in spontaneous and Matri-

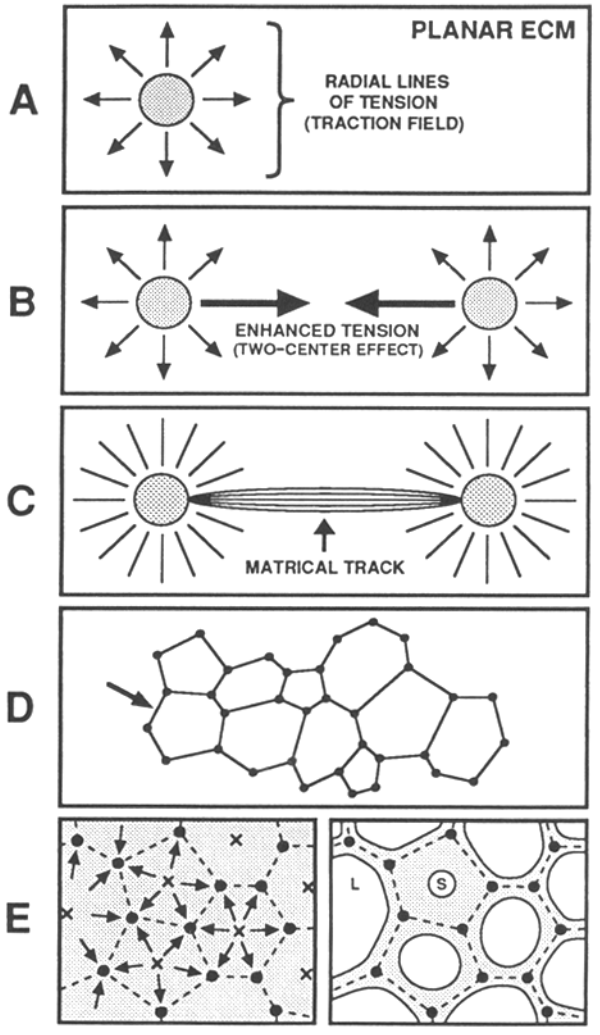

FIG. 8. Cellular traction generates patterns of order in planar ECM in vitro. *A*, viewed from above, a cellular traction center (*shaded circle*) in contact with malleable, planar ECM (*rectangle*) generates radial lines of tension (*arrows*) in the ECM that constitute a traction field. *B*, tension in ECM between adjacent traction centers is enhanced (*large arrows*) as a consequence of the "two-center effect". *C*, fibers of ECM (*black lines*) align along the direction of principal stress. Fibers influenced by the two-center effect align to form a matrical track that connects the traction centers. *D*, traction centers (*small black dots*) arranged in a field on planar ECM become connected by a network of matrical tracks (e.g., *arrow*). *E left*, where planar ECM (*shaded*) is highly malleable, centripetal movement (*arrows*) of ECM to traction centers (*black dots*) results in clearance of ECM from central areas (*x*) that are bordered by two-center effects (*dotted lines*). *E right*, clearance process diagrammed in left panel is manifested as perforations (*white areas*) in the ECM sheet (*shaded*). Perforations are small (*S*) initially, but enlarge with time (*L*). ECM aligned by two-center effects (*dotted lines*) between traction centers (*black dots*) is resistant to cell-generated stresses.

gel models in terms of a two-dimensional organization; therefore, it is likely that ECM scaffolds are typical of angiogenic models in vitro in which planarity is a characteristic.

"Planar angiogenesis in vitro" is unlike angiogenesis in vivo. In the abovementioned culture systems that we refer to collectively as "planar models of angiogenesis in vitro", the cells organize rapidly and precisely into vascular-like networks. It is largely on the basis of the network-like organization of the cells that planar models have been employed in molecular studies of angiogenesis (e.g., 3,10,17–19,23). It seems, however, that planar models lack certain features that are typical of angiogenesis in vivo. For example, during angiogenic neovascularization of tumors and healing wounds, endothelial sprouts branch from extant vasculature and infiltrate the interstitial ECM (2,5,22). The invasive quality of angiogenesis in vivo is poorly reproduced in planar models: cells in the networks display only a limited propensity to burrow into the ECM and, consequently, most of the cells have "outer" surfaces that contact the fluid culture medium. Moreover, planar cellular networks form by tessellation events that occur more or less simultaneously throughout a field of prepositioned cells—a process that differs from the vectorial, invasion/arborization of angiogenic sprouts. During angiogenesis in vivo, endothelial sprouts were reported to form channels or vacuoles that extended the lumens of parent vessels into new vascular branches (5,22). Endothelial cells that comprise planar networks in vitro frequently assume tubular forms; however, the lumens of the tubes are typically filled with ECM (8,9,20,21,25, Vernon and Sage, unpublished observations). It has been suggested (9) that such luminal ECM might mediate the development of tubes by acting as a mandrel around which endothelial cells could wrap. Mandrel-like structures of ECM have not been described in association with invasive angiogenesis in vivo, however. Moreover, the induction of clearance of mandrel-like ECM from cellular tubes that form in vitro has not been reported. With respect to invasion and development of lumens, angiogenic neovascularization is simulated in vitro with greater realism by culture systems in which monolayers of endothelial cells develop branched, tubular invaginations as cells penetrate thick collagen gels in response to phorbol esters or polypeptide growth factors (29,30,32,36). In this type of model, the endothelial tubes exhibit thin walls and wide, patent lumens in the manner of capillaries. Moreover, the lumens extend nearly to the tips of the invading invaginations, a morphology that is characteristic of capillary sprouts that grow in tails of amphibian larvae or rabbit ear wounds (5).

Vasculogenesis and intussusception: a role for planar models? The ability of planar models in vitro to simulate invasive angiogenesis in vivo seems to be limited; therefore, we suggest that in future studies the term "angiogenesis" not be used in connection with planar models. It is important to note, however, that planar models might provide insights into other forms of vascular development in vivo in which planarity is a characteristic. For example, in early chicken and quail embryos, clusters of primordial endothelial cells (angioblasts) that arise within the flat sheet of ECM between the endoderm and splanchnic mesoderm become connected by a planar network of cellular cords that develop lumens and form the paraaortic and vitelline vascular plexuses. This process (7,35,37), termed vasculogenesis, closely resembles the formation of planar cell/ECM networks by subconfluent clusters of endothelial cells that contact layers of ECM in vitro (40). In chicken embryos, traction forces developed by endocardial cells aligned fibers of ECM into linear tracks that projected a considerable distance ahead of the cells (28). The tracks of ECM persisted and were available as pathways by which endocardial cells invaded the developing endocardial cushions (28). Given that tracks of ECM influence cellular migration in the embryo, and given the relative ease with which cells organize sheets of malleable ECM into networks of linear tracks in vitro, the potential exists for a field of angioblastic clusters to apportion the planar ECM of the spanchnopleure into a template that

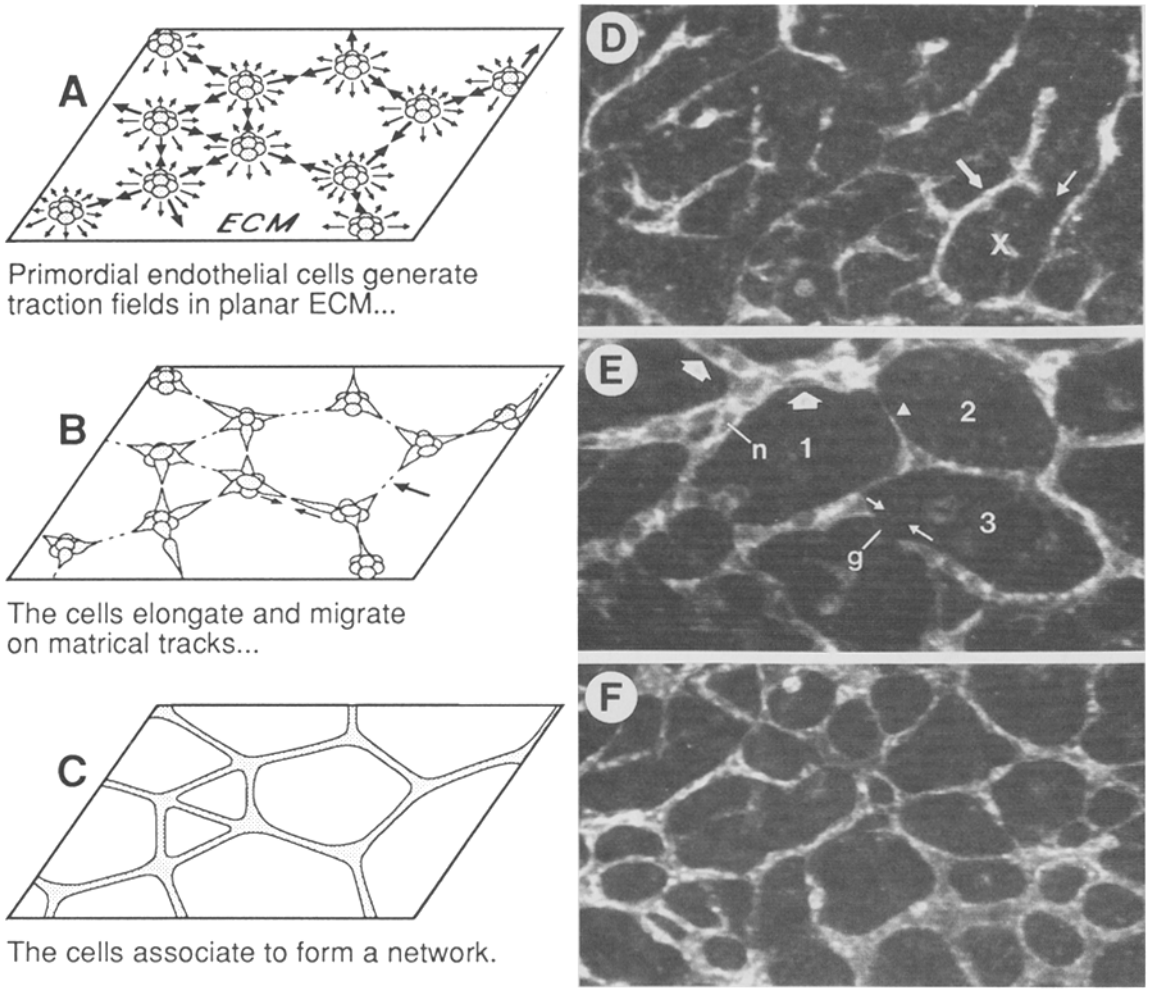

FIG. 9. Hypothetical role of ECM templates in planar vasculogenesis in vivo. *A*, clusters of primordial endothelial cells (*shaded*) generate traction fields (*small arrows*) and two-center effects (*large arrows*) in planar ECM of the splanchnopleure. *B*, cells elongate and migrate from clusters (e.g., *small arrows*) along matrical tracks (*dotted lines* — e.g., *large arrow*). *C*, migratory endothelial cells co-associate to form vascular cords (*shaded*). *D–F*, arrangement of primordial endothelial cells in the developing para-aortic vasculature of early quail embryos is revealed by QH1 immunofluorescence and laser confocal microscopy. *D*, endothelial cords (e.g., *thick arrow*) in a 6-somite embryo form planar polygons that lack complete cellular boundaries and which resemble early stages of spontaneous network formation in vitro (e.g., Fig. 1 *A,B*). Geometric center (*X*) of one polygon is shown. *Note* gap (*thin arrow*) in one side of the polygon. *E*, 6-somite embryo in which vascular tessellation is more advanced. Geometric centers of three vascular polygons are indicated (*1, 2,* and *3*). Polygon 3 has an acellular gap (*g*) with the potential for closure by migration (*small arrows*) of endothelial cells along a matrical track (e.g., as in *B*). An initial stage of network closure is represented by the thin, cellular extension (*arrowhead*) that separates polygon 1 from polygon 2. Thicker, multicellular cords (*large arrows*) comprise areas of greater maturity. Nuclei (*n*) of endothelial cells appear as dark ovals. *F*, in an 8-somite embryo, most vascular polygons have complete cellular boundaries. *E* is ×290; *D,F* are ×145.

influences vascular architecture (Fig. 9 *A–C*). Indeed, we find that the cytoarchitecture of para-aortic vasculogenesis in quail embryos is consistent with a planar, traction/template model (Fig. 9 *D–F*).

Recent observations by Burri (4) suggest that the reorganization of planar vascular sheets might be relevant to the growth of extant vasculature. Analyses by SEM of plastic castings of capillaries within growing rat lungs revealed that the vascular beds were comprised of networks of tubes that intermingled with flat, sheetlike vessels. The vascular sheets were perforated by circular openings (filled with ECM in vivo) of various sizes that, in some cases, were less than 1 μm in diameter. Similar openings were observed in capillary networks of the chorioallantoic membrane of the developing chicken. Burri (4) has proposed that the repeated generation and enlargement of the openings would convert vascular sheets into a network of tubes—a process referred to as growth (i.e. remodeling) by intussusception. Reorganization by intussusception is a characteristic of the planar models we have examined: sheetlike areas of cells or ECM or both are often converted into networks of cords as circular perforations form and enlarge (e.g., Figs. 7 and 8 *E*). Observations indicate that the circular perforations are punctate mechanical failures that enlarge as the cell/ECM sheets are maintained in a state of tension by forces of cellular traction (39,40, present study). It will prove interesting, in future studies, to determine the degree to which pattern-generating processes that typify planar endothelial cultures in vitro are relevant to the development of vasculature in vivo.

Acknowledgments

We thank Dr. May J. Reed (Dept. of Medicine, University of Washington) for her assistance in the isolation of the BAEC clones. This work was supported by grants HL 18645, HD 25059, HD 12629, and GM 40711 from the National Institutes of Health, Bethesda, MD.

References

1. Asaga, H.; Kikuchi, S.; Yoshizato, K. Collagen gel contraction by fibroblasts requires cellular fibronectin but not plasma fibronectin. Exp. Cell Res. 193:167–174; 1991.
2. Ausprunk, D. H.; Folkman, J. Migration and proliferation of endothelial cells in preformed and newly formed blood vessels during tumor angiogenesis. Microvasc. Res. 14:53–65; 1977.
3. Battegay, E. J.; Rupp, J.; Iruela-Arispe, L., et al. PDGF-BB modulates endothelial proliferation and angiogenesis in vitro via PDGF β-receptors. J. Cell Biol. 125:917–928; 1994.
4. Burri, P. H. Intussusceptive microvascular growth, a new mechanism of capillary network formation. In: Steiner, R.; Weisz, P. B.; Langer, R., eds. Angiogenesis. Basel: Birkhäuser Verlag; 1992:32–39.
5. Clark, E. R.; Clark, E. L. Microscopic observations on the growth of blood capillaries in the living mammal. Am. J. Anat. 64:251–301; 1939.
6. Cotta-Pereira, G.; Sage, H.; Bornstein, P., et al. Studies of morphologically atypical ("sprouting") cultures of bovine aortic endothelial cells. Growth characteristics and connective tissue protein synthesis. J. Cell. Physiol. 102:183–191; 1980.
7. Drake, C. J.; Davis, L. A.; Little, C. D. Antibodies to β_1-integrins cause alterations of aortic vasculogenesis, *in vivo*. Dev. Dynam. 193:83–91; 1992.
8. Feder, J.; Marasa, J. C.; Olander, J. V. The formation of capillary-like tubes by calf aortic endothelial cells grown *in vitro*. J. Cell. Physiol. 116:1–6; 1983.
9. Folkman, J.; Haudenschild, C. Angiogenesis *in vitro*. Nature 288:551–556; 1980.
10. Grant, D. S.; Tashiro, K.-I.; Segui-Real, B., et al. Two different laminin domains mediate the differentiation of human endothelial cells into capillary-like structures. Cell 58:933–943; 1989.
11. Guidry, C.; Hook, M. Endothelins produced by endothelial cells promote collagen gel contraction by fibroblasts. J. Cell Biol. 115:873–880; 1991.
12. Gullberg, D.; Tingstrom, A.; Thuresson, A.-C., et al. β_1 Integrin-mediated collagen gel contraction is stimulated by PDGF. Exp. Cell Res. 186:264–272; 1990.
13. Harris, A. K.; Stopak, D.; Warner, P. Generation of spatially periodic patterns by a mechanical instability: a mechanical alternative to the Türing model. J. Embryol. Exp. Morphol. 80:1–20; 1984.
14. Harris, A. K.; Stopak, D.; Wild, P. Fibroblast traction as a mechanism for collagen morphogenesis. Nature 290:249–251; 1981.
15. Harris, A. K.; Wild, P.; Stopak, D. Silicone rubber substrata: a new wrinkle in the study of cell locomotion. Science 208:177–179; 1980.
16. Ingber, D. E.; Folkman, J. Mechanochemical switching between growth and differentiation during fibroblast growth factor-stimulated angiogenesis *in vitro*: Role of extracellular matrix. J. Cell Biol. 109:317–330; 1989.
17. Iruela-Arispe, M. L.; Diglio, C. A.; Sage, E. H. Modulation of extracellular matrix proteins by endothelial cells undergoing angiogenesis *in vitro*. Arterioscl. Thromb. 11:805–815; 1991.
18. Iruela-Arispe, M. L.; Hasselaar, P.; Sage, H. Differential expression of extracellular proteins is correlated with angiogenesis *in vitro*. Lab. Invest. 64:174–186; 1991.
19. Iruela-Arispe, M. L.; Sage, E. H. Endothelial cells exhibiting angiogenesis *in vitro* proliferate in response to TGF-β1. J. Cell. Biochem. 52:414–430; 1993.
20. Jackson, C. J.; Jenkins, K. L. Type I collagen fibrils promote rapid vascular tube formation upon contact with the apical side of cultured endothelium. Exp. Cell Res. 192:319–323; 1991.
21. Jackson, C. J.; Jenkins, K.; Schrieber, L. Possible mechanisms of type I collagen-induced vascular tube formation. In: Steiner, R.; Weisz, P. B.; Langer, R., eds. Angiogenesis. Basel: Birkhäuser Verlag; 1992:198–204.
22. Konerding, M. A.; vanAckern, C.; Steinberg, F., et al. Combined morphological approaches in the study of network formation in tumor angiogenesis. In: Steiner, R.; Weisz, P. B.; Langer, R., eds. Angiogenesis. Basel: Birkhäuser Verlag; 1992:40–58.
23. Kubota, Y.; Kleinman, H. K.; Martin, G. R., et al. Role of laminin and basement membrane in the morphological differentiation of human endothelial cells into capillary-like structures. J. Cell Biol. 107:1589–1598; 1988.
24. Laemmli, U. K. Cleavage of structural proteins during the assembly of the head of bacteriophage T4. Nature 227:680–685; 1970.
25. Maciag, T.; Kadish, J.; Wilkins, L., et al. Organizational behavior of human umbilical vein endothelial cells. J. Cell Biol. 94:511–520; 1982.
26. Madri, J. A.; Pratt, B. M. Endothelial cell-matrix interactions: *in vitro* models of angiogenesis. J. Histochem. Cytochem. 34:85–91; 1986.
27. Madri, J. A.; Williams, S. K.; Wyatt, T., et al. Capillary endothelial cell cultures: phenotypic modulation by matrix components. J. Cell Biol. 97:153–165; 1983.
28. Markwald, R. R.; Fitzharris, T. P.; Bolender, D. L., et al. Structural analysis of cell:matrix association during the morphogenesis of atrioventricular cushion tissue. Dev. Biol. 69:634–654; 1979.
29. Montesano, R.; Orci, L. Tumor-promoting phorbol esters induce angiogenesis *in vitro*. Cell 42:469–477; 1985.
30. Montesano, R.; Orci, L. Phorbol esters induce angiogenesis *in vitro* from large-vessel endothelial cells. J. Cell. Physiol. 130:284–291; 1987.
31. Montesano, R.; Orci, L.; Vassalli, P. *In vitro* rapid organization of endothelial cells into capillary-like networks is promoted by collagen matrices. J. Cell Biol. 97:1648–1652; 1983.
32. Montesano, R.; Pepper, M. S.; Orci, L. Paracrine induction of angiogenesis *in vitro* by Swiss 3T3 fibroblasts. J. Cell Sci. 105:1013–1024; 1993.
33. Opas, M. Expression of the differentiated phenotype by epithelial cells *in vitro* is regulated by both biochemistry and mechanics of the substratum. Dev. Biol. 131:281–293; 1989.
34. Pardanaud, L.; Altmann, C.; Kitos, P., et al. Vasculogenesis in the early quail blastodisc as studied with a monoclonal antibody recognizing endothelial cells. Development 100:339–349; 1987.
35. Patten, B. M. Early embryology of the chick. New York: McGraw-Hill; 1971.
36. Pepper, M. S.; Ferrara, N.; Orci, L., et al. Potent synergism between vascular endothelial growth factor and basic fibroblast growth factor in the induction of angiogenesis in vitro. Biochem. Biophys. Res. Commun. 189:824–831; 1992.
37. Poole, T. J.; Coffin, J. D. Developmental angiogenesis: quail enbryonic vasculature. Scanning Microsc. 2:443–448; 1988.
38. Reed, M. J.; Vernon, R. B.; Abrass, I. B., et al. TGF-β1 induces the expression of type I collagen and SPARC, and enhances contraction of collagen gels, by fibroblasts from young and aged donors. J. Cell. Physiol. 158:169–179; 1994.
39. Stopak, D.; Harris, A. K. Connective tissue morphogenesis by fibroblast traction. Dev. Biol. 90:383–398; 1982.
40. Vernon, R. B.; Angello, J. C.; Iruela-Arispe, M. L., et al. Reorganization of basement membrane matrices by cellular traction promotes the formation of cellular networks *in vitro*. Lab. Invest. 66:536–547; 1992.
41. Vernon, R. B.; Sage, H. The calcium-binding protein SPARC is secreted by Leydig cells and Sertoli cells of the adult mouse testis. Biol. Reprod. 40:1329–1340; 1989.
42. Weiss, P. *In vitro* experiments on the factors determining the course of the outgrowing nerve fiber. J. Exp. Zool. 68:393–448; 1934.